

PCCP

Accepted Manuscript



This is an *Accepted Manuscript*, which has been through the Royal Society of Chemistry peer review process and has been accepted for publication.

Accepted Manuscripts are published online shortly after acceptance, before technical editing, formatting and proof reading. Using this free service, authors can make their results available to the community, in citable form, before we publish the edited article. We will replace this *Accepted Manuscript* with the edited and formatted *Advance Article* as soon as it is available.

You can find more information about *Accepted Manuscripts* in the [Information for Authors](#).

Please note that technical editing may introduce minor changes to the text and/or graphics, which may alter content. The journal's standard [Terms & Conditions](#) and the [Ethical guidelines](#) still apply. In no event shall the Royal Society of Chemistry be held responsible for any errors or omissions in this *Accepted Manuscript* or any consequences arising from the use of any information it contains.



PCCP

ARTICLE

Molecular Simulations of Cytochrome c Adsorption on Positively Charged Surfaces: The Influence of Anion Type and Concentration

Chunwang Peng,^a Jie Liu,^{a,b} Yun Xie^c and Jian Zhou*^a

Received xxx January 2016,
Accepted xxx February 2016

DOI: 10.1039/x0xx00000x

www.rsc.org/pccp

Contradictory results have been reported regarding to Cytochrome c (Cyt-c) adsorption onto the positively charged SAMs, and the role of small anions played in the adsorption is still unclear. In this work, the adsorption of Cyt-c on the amino-terminated SAM (NH₂-SAM) and the effect of chloride and phosphate ions on the adsorption were studied using molecular dynamics simulations. The results reveal that Cyt-c could not stably adsorb onto the surface even at a relatively high ionic strength when chloride ions were added; while phosphate ions could promote its adsorption. Under a low phosphate concentration, Cyt-c can adsorb on the NH₂-SAM mainly with two opposite orientations. One is similar to that characterized in the experiments for Cyt-c adsorbed on the NH₂-SAMs, which points the heme group far away from the surface. The other orientation is similar to that for Cyt-c on the carboxyl-terminated SAMs. In the latter case, phosphate ions formed a distinct counterion layer near the surface and overcompensated the positive charge of the surface. Further analysis show that chloride ions have no significant tendency to aggregate near the NH₂-SAM surface and cannot shield the electrostatic repulsion between Cyt-c and the surface; while the phosphate ions can easily adsorb onto the surface and bind specifically to certain lysine residues of Cyt-c, which mediate its adsorption. At a high phosphate concentration, the phosphate and sodium ions will aggregate to form clusters, which results in random adsorption orientation. This work may provide some guidance for the design of Cyt-c-based bioelectronic devices and controlled enzyme immobilization.

1. Introduction

The direct electron transfer (ET) between redox protein and the electrode surfaces plays a significant role in the development of new enzymatic biofuel cells, bioelectronic devices, biosensors, and so on.¹⁻⁶ Cytochrome c (Cyt-c) is a typical redox protein, which is often applied to the investigation of the structure, kinetics, thermodynamics, and direct ET reactions of heme-protein. Clarifying the binding ability of Cyt-c with different kinds of surfaces and characterizing its redox properties in these complexes will contribute to a better understanding of the interactions of Cyt-c with its biological partners and with the building blocks involved in biomimetic and technological devices.⁷

Studies have shown that the direct adsorption of Cyt-c on a bare electrode (e.g. Pt, Hg, Au, or Ag) surface hampers the ET between Cyt-c and the electrode.^{8,9} Efforts to improve the ET efficiency have led to the use of self-assembled monolayers (SAMs) to modify the electrode surface. Cyt-c carries a net positive charge at neutral pH, and there is a positively

charged lysine-rich domain surrounding the partially exposed heme crevice,⁹⁻¹¹ which is involved in the electrostatic binding to its natural redox partners in the mitochondrial ET chain. Thus, a commonly used strategy is to electrostatically immobilize Cyt-c on SAMs terminated with negatively charged functional groups. The adsorption of Cyt-c on carboxyl-terminated SAM (COOH-SAM) has been extensively studied both experimentally¹⁰⁻¹³ and theoretically.¹⁴⁻¹⁹ The results show that the adsorption leads to the heme edge being close and nearly perpendicular to the surface.^{11, 12, 18, 19}

It is supposed that the heme edge of Cyt-c be close to the electrode surface to allow for a fast ET.¹⁸ Recently, it is suggested that the ET of the immobilized Cyt-c be controlled by the interplay between protein dynamics and tunneling probabilities.¹⁹

Surprisingly, it has been reported that Cyt-c is also able to adsorb onto the positively charged surfaces, such as SAMs terminated with amino (–NH₂) or trimethylammonium (–N⁺(CH₃)₃) group, and exhibited different electrochemical response.²⁰ The orientation of Cyt-c on the positively charged amino-terminated SAMs (NH₂-SAMs) has also been probed by different techniques. Yu and Golden¹² applied surface-enhanced Raman scattering (SERS) to probe the orientations of Cyt-c on the NH₂-SAMs and found that the heme group was pointed away from the surface. Baio et al.¹³ probed the orientation of Cyt-c electrostatically immobilized onto both amino (–NH₂) and carboxyl (–COOH) functionalized gold by time of flight secondary ion mass spectrometry (ToF-SIMS)

^a School of Chemistry and Chemical Engineering, Guangdong Provincial Key Lab for Green Chemical Product Technology, South China University of Technology, Guangzhou, 510640, P. R. China. E-mail: jianzhou@scut.edu.cn

^b Key Laboratory for Green Chemical Process of Ministry of Education, School of Chemical Engineering and Pharmacy, Wuhan Institute of Technology, Wuhan 430073, China

^c School of Chemistry and Chemical Engineering, Guangdong Pharmaceutical University, Guangzhou 510006, P. R. China

† Electronic supplementary information (ESI) available. See DOI: 10.1039/x0xx0000x

and sum frequency generation (SFG) spectroscopy. Their results showed that Cyt-c had opposite orientations on the two different surfaces; the heme group is pointed away from the positively charged surface. However, it is known to us that both Cyt-c and NH₂-SAM are positively charged at pH 7, and no protein adsorption is expected. Some similar results have also been reported. For example, Jensen et al.²¹ found that no Cyt-c adsorption was detected on cysteamine SAMs. Recently, Capdevila et al.⁷ employed surface-enhanced resonance Raman (SERR) spectro-electrochemistry to study the adsorption of Cyt-c on NH₂-SAMs. Their results showed that Cyt-c is incapable of binding efficiently to NH₂-SAMs in pure water or with the addition of 10 mM KCl, KNO₃, K₂SO₄, TrisCl buffer or HEPES buffer.⁷ However, the inorganic phosphate (Pi) and ATP anions could mediate Cyt-c's binding and preserve its native structure, resulting in an average orientation that is beneficial to direct ET.⁷

Although some experiments can provide structural, electronic, and dynamic information simultaneously, in situ detection of conformation and orientation changes of proteins occurring at the molecular level is still technically challenging. Molecular simulations are well-suited to study protein adsorption behavior on surfaces and provide molecular level information. Molecular simulations are well-suited to study the behavior of protein adsorption on surfaces at the molecular level.¹⁸ So far, some molecular dynamics (MD) simulation studies of Cyt-c adsorption on solid surfaces have been reported.^{14-19, 22-24} These works mainly focus on the adsorption of Cyt-c on the negatively charged SAMs.¹⁴⁻¹⁹ Recently, MD simulations regarding to the interaction of Cyt-c with monolayer-protected metal nanoparticle surfaces,²² zwitterionic phosphorylcholine SAMs²³ and a bare gold surface²⁴ have been performed.

As discussed above, both the adsorption of Cyt-c on positively charged and negatively charged surfaces can undergo reversible ET. What is the difference between the underlying mechanisms? For the adsorption of Cyt-c on the positively charged surface, different experiments lead to conflicting results. How is Cyt-c adsorbed onto the NH₂-SAM, and what is the role of phosphate played in the adsorption? The current simulation works mainly focus on the adsorption of Cyt-c onto COOH-SAM.¹⁴⁻¹⁹ To the best of our knowledge, no simulation work has been reported for Cyt-c adsorption on the positively charged surface. Furthermore, the role of small counterions played in protein adsorption is rarely taken into consideration in simulations.²³ However, it has been found that ionic strength has significant impact on protein adsorption.²⁵⁻³⁰ For example, the formal potential of immobilized Cyt-c depended on the solution ionic strength.²⁵ A relatively low phosphate concentration (50 mM) alleviated the denaturation of bovine serum albumin and some other proteins at a bare mercury electrode while at higher phosphate concentrations they underwent electric field-driven denaturation.²⁷

In this work, MD simulations were performed to explore the adsorption behavior of Cyt-c on the NH₂-SAM surface. The effects of different anion types (chloride and phosphate

ions) and their concentration on the adsorption were also studied. Firstly, the distribution of the anions around the surfaces of Cyt-c and NH₂-SAM were analyzed. Then, the adsorption orientation and conformation of Cyt-c on NH₂-SAM were studied in detail. Finally, some possible explanations for the contradictory results in the experiments were given.

2. Materials and Methods

2.1. Protein and Surfaces

Cyt-c. The crystal structure of horse heart Cyt-c³¹ (PDB code: 1HRC) obtained from the RCSB (www.rcsb.org) is used in our simulations. It consists of 104 residues and a prosthetic group (heme), with five α -helices and two anti-parallel β -sheets. The overall structure is approximately spherical with a diameter of about 3.4 nm. The heme iron is coordinated with a histidine (His18) and a methionine (Met80), and two vinyl groups of the heme ring are covalently bonded to two cysteines (Cys14 and Cys17) via thioether bonds.³² The protein was studied at physiological conditions, with lysine and arginine residues being protonated, while aspartic acid and glutamic acid residues together with the C-terminus being deprotonated.¹⁸ The N-terminus was acetylated as it presents in the crystal structure. Hydrogen atoms were added by the *pdb2gmx* tool of the GROMACS 4.5.4 package.³³ Heme was treated in the oxidized state³¹ (consistent with the crystal structure); the charge distribution and force field parameters for heme and its linkage with the peptide chain were adopted from Autenrieth et al.'s work.³² The protein contains 1749 atoms bearing a net charge of +7e. The potential parameters for Cyt-c are adopted from the CHARMM27 force field.³⁴

NH₂-SAM. The ($\sqrt{3}\times\sqrt{3}$)R30° lattice structure^{35, 36} was adopted for SAMs of S(CH₂)₁₁NH₂ in all-atom MD simulations. The surface consists of 168 thiol chains with a dimension of 5.994×6.056 nm². Among them, 12 (about 7% dissociation) chains are protonated, representing a surface charge density of 0.05 C/m².^{35, 36} All the sulfur atoms in the SAMs were kept fixed during the simulations. The potential parameters for the SAM are adopted from the CHARMM force field for lipids.³⁷

Phosphate ions. It can be found in the literature³⁸ that the pK_{a2} value of phosphoric acid at 25 °C is 7.21. It indicates that when the pH value of the phosphate buffer saline is 7.21, H₂PO₄⁻ and HPO₄²⁻ prevail in the solution with a same concentration. Therefore, under physiological conditions (pH \approx 7.4), the proportion of HPO₄²⁻/H₂PO₄⁻ should approximate to 1.55:1. However, the ratio between the two ions in real physiological conditions is also correlated with many other factors, such as activity coefficient, temperature and ionic strength.³⁹ Therefore, it is difficult to determine the exact ratio between these two ions. In this work, we suppose the ratio of HPO₄²⁻/H₂PO₄⁻ to be 1:1, so that we can determine which ion is more accounted to the adsorption. The CHARMM atom-type and charge assigned to each atom in phosphate ions, and the force field parameters for phosphate ions⁴⁰⁻⁴² are given in detail in the ESI.†

2.2. Simulation Details

To investigate the adsorption mechanisms of Cyt-c on the NH₂-SAM under different conditions, a total of 31 different systems (for Cyt-c and NH₂-SAM in water, six different initial configurations were chosen for each) have been constructed. The settings for all the simulated systems are listed in Table 1. In the following, we will briefly describe them.

Table 1 Settings for All the Simulated Systems

System	Conc. ^a (M)	H ₂ PO ₄ ⁻ /HPO ₄ ²⁻	Na ⁺ /Cl ⁻	Box size (nm ³)	Time (ns)
Cyt-c in water	0.056	4/4	5/0	6.2×6.2×6.2	40
	0.23	15/15	38/0	6.0×6.0×6.0	
	0.05	0/0	8/20		
NH ₂ -SAM in water	0.15	0/0	25/37	5.99×6.06×8.0	40
	0.058	5/5	3/0		
	0.15	13/13	27/0		
	0.15	13/13	52/25		
Cyt-c and NH ₂ -SAM in water	0.05	0/0	8/27	5.99×6.06×8.0	80
	0.15	0/0	25/44		
	0.058	5/5	0/4		
	0.17	15/15	26/0		

^a Conc. refers to anion concentration

Cyt-c in water. Here, the binding behaviour of phosphates ions with Cyt-c was studied. First, the Cyt-c molecule was put into the centre of the cubic boxes. Then, the boxes were solvated with TIP3P water.⁴³ It is suggested that the CHARMM TIP3P model (also known as the TIPS3P model) with Lennard-Jones interactions on the hydrogen atoms should be used for lipids simulations.⁴⁴ However, it has been proved that simulations for protein systems with the standard TIP3P model have a minimal impact upon the protein dynamics when compared with the CHARMM TIP3P model.⁴⁵ In addition, this work focuses on the protein adsorption behaviour instead of the membrane properties. As far as we know, the standard TIP3P water model has also been used in some previous works^{17, 30} for MD simulations of protein adsorption on the charged COOH- and NH₂-SAM surfaces in both low and relatively high ionic strength conditions (such as 0.15-0.17M physiological condition, just like ours). Furthermore, the CHARMM TIP3P water model is about two times slower than the standard TIP3P model,⁴⁵ thus we think that it is more efficient to use the latter. Finally, phosphate and sodium ions were added to neutralize the systems with the anion concentration (Conc.) to be 0.056 M or 0.23 M (see Table 1). Each of the simulations was conducted in the NPT ensemble for 40 ns. The temperature was controlled at 300 K via a Nosé-Hoover thermostat⁴⁶ and the pressure was coupled to 1 bar by using an isotropic Parrinello-Rahman barostat.⁴⁷ During the simulations, the positions of the

backbone atoms of Cyt-c were restrained to obtain accurate number-density maps of phosphates ions around the protein.

NH₂-SAM in water. Here, the adsorption behavior of chloride and phosphate ions on the NH₂-SAM was investigated. First, the NH₂-SAM surface was placed in the bottom of the simulation boxes. Then, the boxes were solvated with TIP3P water.⁴³ Finally, sodium ions, and phosphate and/or chloride ions were added to neutralize the systems with different anion concentrations (see Table 1). Each of the simulations was conducted for 40 ns. During the simulations, all the sulfur atoms in SAMs were kept fixed.

Cyt-c and NH₂-SAM in water. To explore the adsorption mechanisms of Cyt-c on the NH₂-SAM, six different orientations (as shown in Fig. 1a-f, equivalent to the six faces of a box) were chosen as the starting points for each system. Among them, two are the adsorption orientations of Cyt-c on the NH₂-SAM (Fig. 1a) and COOH-SAM (Fig. 1d), as reported in the experiments^{12, 13} and our Parallel Tempering Monte Carlo simulations.²⁴ Initially, the minimum distance between Cyt-c and the surface is greater than 0.6 nm. Water molecules described by TIP3P model⁴³ were filled in a box of 5.994×6.056×8.0 nm³. Chloride and/or sodium ions were added to neutralize the systems with the anion concentration to be 0.05 M or 0.15 M. For systems containing phosphate ions, 5 or 15 pairs of H₂PO₄⁻/HPO₄²⁻ were added.

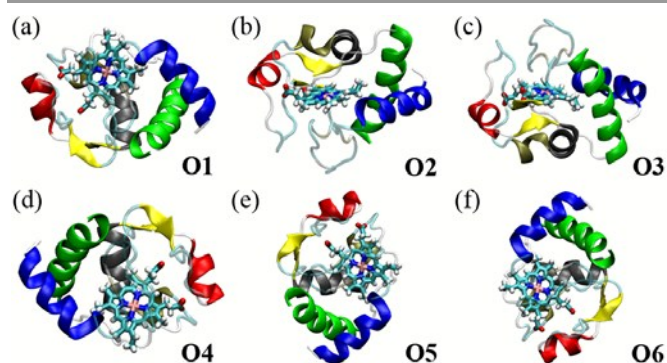


Fig. 1 The six initial orientations of Cyt-c for MD simulations. Cyt-c is displayed in NewCartoon mode and the heme group is represented in Licorice mode.

The temperature was controlled at 300 K via a Nosé-Hoover thermostat.⁴⁶ Bonds containing hydrogen atoms were constrained using the LINCS algorithm.⁴⁸ A switched potential was adopted to calculate the nonbonded interactions with a switching function between 0.9 and 1 nm. Electrostatic interactions were calculated by the particle mesh Ewald (PME) method⁴⁹ in 3dc geometry⁵⁰ with a cutoff distance of 1.1 nm. Periodic boundary conditions were applied only in the x and y directions. Two virtual hard walls (represented by water oxygen atoms) were set at both the top and the bottom of the simulation box to prevent the water molecules from penetrating into the vacuum layer, and the scaling factor for the z direction for Ewald summation was 3, which is a routine implemented in the GROMACS 4.5.4 package³³ for the simulations of charged slab geometry. First, the systems were minimized by the steepest descent method.⁸⁰ Then, a 100 ps NVT equilibration with a position restraint on

heavy atoms of Cyt-c was conducted for each system. Successively, the pressure was weakly coupled using a semi-isotropic Parrinello-Rahman barostat⁴⁷ in which the lateral pressure equals 0 due to the rigid sulfur atoms of the surface and the perpendicular pressure equals 1 bar for 100 ps to equilibrate the volume of the box. Finally, each system was run for 80 ns MD simulations in the NVT ensemble with a time step of 2 fs. The trajectories were visualized by the Visual Molecular Dynamics (VMD) program.⁵¹

3. Results and Discussion

3.1. Distribution of phosphate ions around Cyt-c

To investigate the binding behavior of phosphates ions with Cyt-c, MD simulations of Cyt-c in two different phosphate buffer solutions (Table 1) were conducted. The two-dimensional (2D) number-density maps of phosphate in the simulation box were calculated. They are shown in Fig. 2a and 2c. The corresponding equilibrium snapshots of phosphate around Cyt-c are shown in Fig. 2b and 2d. As can be seen from Fig. 2, the phosphate ions are inclined to bind four patches of Cyt-c, which are close to the positively charged Lys7 and Lys100 (I), Lys25 and Lys27 (II), Lys39 and Lys60 (III), Lys13, Lys86 and Lys87 (IV). It is clear that the phosphate ions formed cluster with sodium ions at a high ion concentration. With a careful observation, we can find that the position of the cluster (V) has no direct link with the four binding patches.

We also calculated the radial distribution function of the phosphorus atom around the nitrogen atom of the side chain of lysine residues for the phosphate concentration of 0.23M, and the results with distribution being the top ten are shown in Fig. 3. It is obvious that the phosphate is more inclined to bind with Lys86 and Lys87 (IV), which is in accordance with

previous experimental results⁵². The binding of phosphate to this site has been proved to be very strong and the bound phosphate cannot be displaced by carbonate.⁵² The phosphate ions can also increase the stability of the closed heme crevice structure of Cyt-c.⁵²

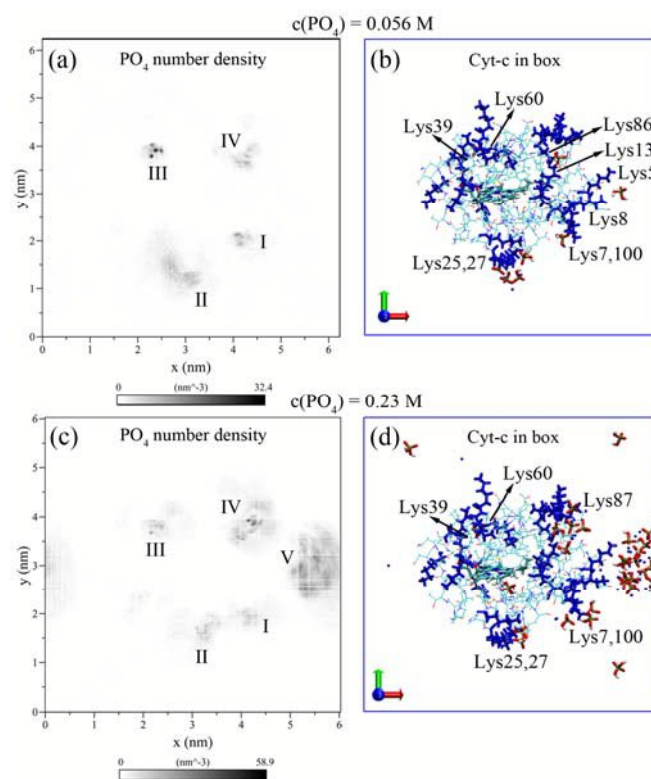


Fig. 2 The two-dimensional number-density maps of phosphate in the simulation box and the corresponding equilibrium snapshots of phosphate around Cyt-c. Cyt-c is displayed in Line mode; the heme, lysine residues (colored in blue), sodium and phosphate ions are represented in Licorice mode.

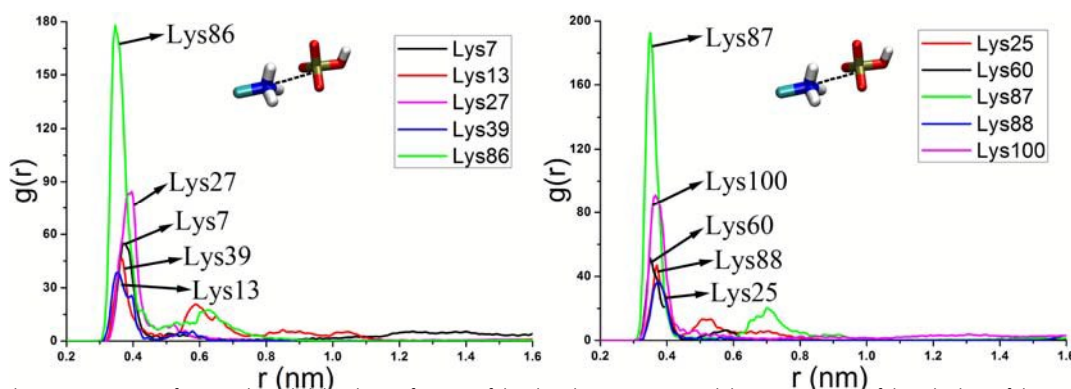


Fig. 3 For the phosphate concentration of 0.23M, the radial distribution function of the phosphorus atom around the nitrogen atom of the side chain of the top ten lysine residues.

3.2. Distribution of anions near the NH₂-SAM surface

To investigate the adsorption behavior of anions on the NH₂-SAM surface, MD simulations of NH₂-SAM surface in aqueous environment with chloride and/or phosphate ions of different concentrations (Table 1) were conducted. The density profiles of chloride and phosphate ions along the surface normal of NH₂-SAM were calculated. The results are shown in Fig. 4. The corresponding equilibrium snapshots of

the ions in the simulation boxes are displayed in the insets of Fig. 4.

As can be seen from Fig. 4a, the chloride ions do not significantly adsorb onto the positively charged NH₂-SAM surface and the increase of ion concentration has little impact on the distribution of chloride ions. The similar phenomenon has also been found in a previous work for the weakly charged NH₂-SAM.³⁰ As the surface charge increases, the

chloride ion will have a relatively stronger tendency to adsorb on the $\text{NH}_2\text{-SAM}$.³⁰ However, it is obvious that phosphate ions are more inclined to bind to the $\text{NH}_2\text{-SAM}$ surface. When the phosphate concentration is low (Fig. 4b), HPO_4^{2-} has a stronger affinity to the surface than H_2PO_4^- . This may be ascribed to the bearing of more negative charges of HPO_4^{2-} than H_2PO_4^- . The density profiles of H_2PO_4^- and Cl^- are similar, which indicates that the binding affinity of anions to the positively charged $\text{NH}_2\text{-SAM}$ surface is mainly determined by their valence states. At a relatively high concentration (Fig. 4c), H_2PO_4^- , HPO_4^{2-} and Na^+ will aggregate to form clusters structure with a specific arrangement (with HPO_4^{2-} and Na^+ inside and H_2PO_4^- outside), which makes H_2PO_4^- to be closer to the surface. As HPO_4^{2-} can simultaneously form salt bridges with two sodium ions, this may be the cause of the formation of clusters with specific structures. When both the chloride and phosphate ions are added to the solution with a relatively high concentration (Fig. 4d), the results are almost the superposition of Fig. 4a and Fig. 4c, which indicates that the addition of chloride ions does not influence the adsorption of phosphate ions onto the $\text{NH}_2\text{-SAM}$ surface.

As the presence of multivalent ions in phosphate buffer, which can form salt bridge with sodium ions, the phosphate and sodium ions can aggregate to form clusters. In experiments, it had also been proved that the presence of calcium phosphate clusters from 0.7 to 1.0 nm in a simulated body fluid (2.5 mM CaCl_2 , 1 mM $\text{K}_2\text{HPO}_4\cdot 3\text{H}_2\text{O}$, 140 mM NaCl buffered at pH 7.4) by using the intensity-enhanced dynamic light-scattering technique.⁵³ They also observed that although the calcium phosphate clusters were present in the fluid, no spontaneous precipitation occurred from the fluid even after the fluid had been kept at room temperature for 5 months.⁵³ In their another work, they found that when the concentration of KCl was less than 100 mM, the calcium phosphate clusters in the solution immediately aggregated.⁵⁴ The similar phenomenon has also been found in our MD simulations (as shown in Fig. 4c and Fig. 4d). That is, a large cluster forms when no chloride ion is added, while multiple clusters with similar sizes form when the chloride concentration is high (150 mM).

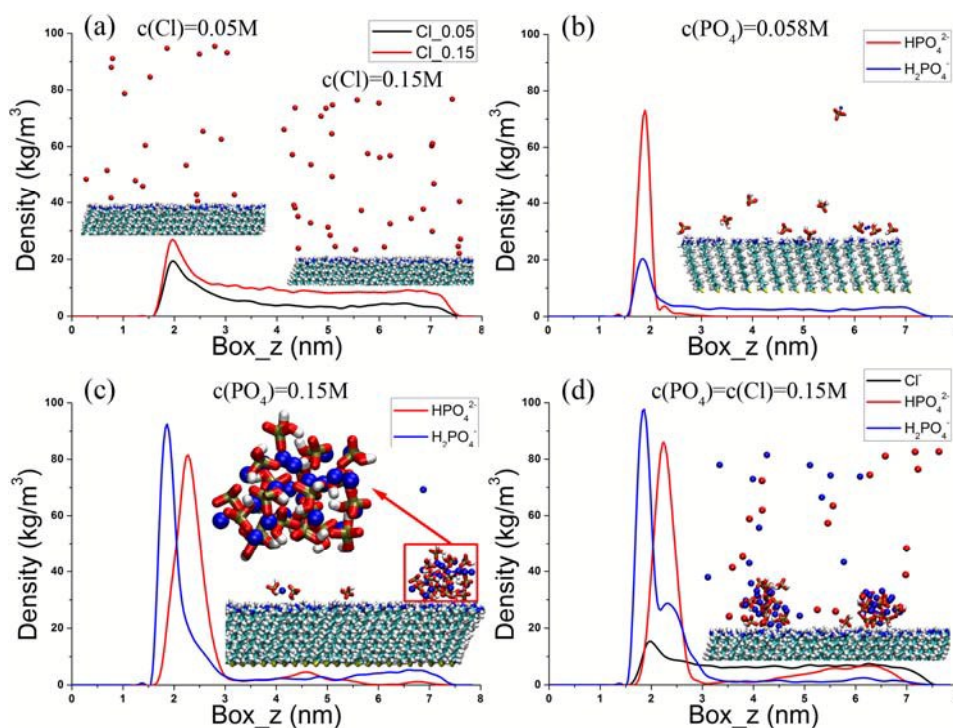


Fig. 4 Density profiles of chloride and phosphate ions along the surface normal of $\text{NH}_2\text{-SAM}$. The insets display the corresponding equilibrium snapshots of the ions in the simulation boxes. For clarity, water and part of the $\text{NH}_2\text{-SAM}$ are not shown.

3.3. Adsorption of Cyt-c onto the $\text{NH}_2\text{-SAM}$ surface

Adsorption Orientation. To inspect the adsorption behaviors of Cyt-c on the $\text{NH}_2\text{-SAM}$ surface, 24 different systems were constructed. That is, 6 initial orientations, 2 different ion types, and 2 ion concentrations. All these simulations were performed for 80 ns. From our simulations, we find that Cyt-c can hardly adsorb on $\text{NH}_2\text{-SAM}$ with the addition of chloride ion, regardless of its concentration. Here, we have calculated the minimum distance between Cyt-c and the $\text{NH}_2\text{-SAM}$

surface. The typical time evolutions of these distances for adding of different concentrations of chloride and phosphate ions are shown in Fig. 5. As can be seen, when 0.05 M chloride is added, Cyt-c can only adsorb on the surface at the time of ~ 30 ns and then leave away from the surface without any further approaching. When 0.15 M chloride is added, Cyt-c moves close and away from the surface, exhibiting reversible adsorption. These may be ascribed to the shielding of the electrostatic repulsion between Cyt-c and the $\text{NH}_2\text{-SAM}$

caused by the high ionic strength. As the chloride does not have a propensity to adsorb on the surface, it cannot form an

effective counterion layer⁵⁵ at the solid-liquid interface. Therefore, Cyt-c cannot stably adsorb on the surface.

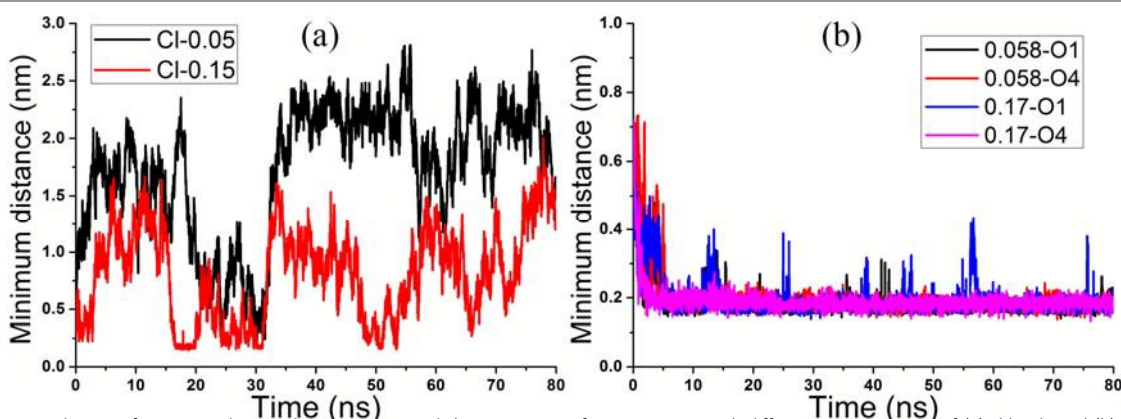


Fig. 5 Typical time evolutions of minimum distance between Cyt-c and the NH₂-SAM surface in systems with different concentrations of (a) chloride and (b) phosphate ions.

When phosphate ions are added, Cyt-c can easily adsorb onto the NH₂-SAM surface for both low and high ion concentrations (Fig. 5b). The final snapshots for MD simulations of Cyt-c adsorbed on the NH₂-SAM surface with the addition of different concentrations of phosphate ions are shown in Fig. 6. To explain that the final orientations are independent on the initial orientations, we have calculated the evolution of the heme tilt angle for Cyt-c adsorbed on the NH₂-SAM surfaces, the results are shown in Figure S2 (ESI[†]). As can be seen, although the simulations for Cyt-c adsorption

on the NH₂-SAM are relatively short, almost all these simulations have reached equilibrium. The results show that, though starting from six different orientations, five (O1, O2, O3, O5 and O6) of them reached a similar final adsorption configuration (see Fig. 6a-f) with similar heme tilt angles for the low phosphate concentration, while several different heme tilt angles reached for the high phosphate concentration. These suggest that the adsorption is reflective of equilibrium propensity rather than highly correlated with the initial orientations.

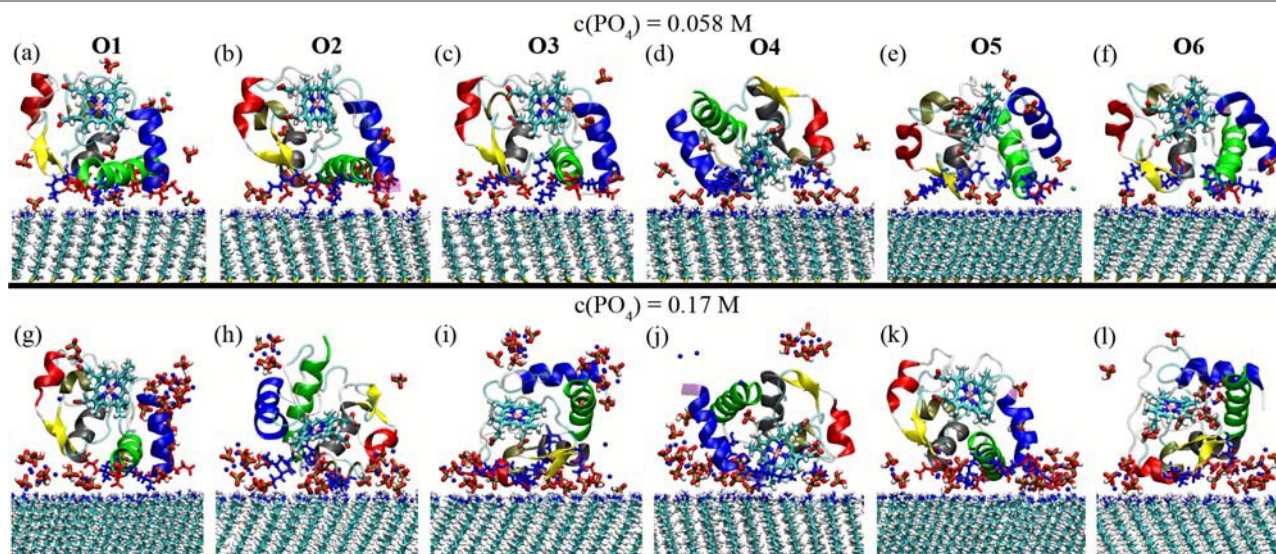


Fig. 6 Final snapshots for MD-simulations of Cyt-c adsorbed on the NH₂-SAM surface under different phosphate concentrations. The top and bottom row are the corresponding adsorption configurations starting from the six initial orientations (as shown in Fig. 1) for 0.058 M and 0.17 M phosphate, respectively. Cyt-c is displayed in NewCartoon mode; the heme, ions, NH₂-SAM surface, and charged residues within 3.5 Å from the surface are represented in Licorice mode. Water molecules are not shown for clarity.

To choose the most stable adsorption configurations for further analyses, the interaction energies between Cyt-c and the NH₂-SAM surface for all these simulations were calculated, and the results are shown in Table S5 (ESI[†]). As can be seen, the two typical adsorption configurations starting from O1 and O4 have the strongest interactions between Cyt-c and the NH₂-SAM surface. As can be seen from Fig. 1 and Fig. 6, for the initial orientations O1 and O4, which are reported in the experiments^{12, 13} for Cyt-c on the NH₂-SAM (Fig. 1a) and

COOH-SAM (Fig. 1d), Cyt-c can quickly and stably adsorb on the surface (Fig. 5b) with little change of its orientation. With a careful observation, we find that the two orientations are exactly opposite to each other, with the heme group being close to or far away from the surface. The similar results have also been found in a previous work for the adsorption of the negatively charged feruloyl esterase on the COOH-SAM.³⁰ It is obvious that Cyt-c mainly adsorb on the NH₂-SAM with the heme group far away from the surface under low phosphate

concentration, which indicates that the adsorption orientation is dominant by the dipole direction.^{18, 24, 29, 30, 35, 36, 56}

This orientation is consistent with those characterized by SERS¹² and ToF-SIMS¹³ for Cyt-c adsorbed on the NH₂-SAM. At the high phosphate concentration, H₂PO₄⁻, HPO₄²⁻, and Na⁺ will aggregate to form a cluster structure, which leads to the adsorption orientation of Cyt-c being relatively random. From Table S5 (ESI[†]), we can also find that higher phosphate concentration can decrease the interactions between Cyt-c and the NH₂-SAM surface.

To further investigate the adsorption of Cyt-c on the NH₂-SAM at the presence of low phosphate concentration, the orientation distribution of Cyt-c adsorbed on the surface, and density profile of phosphate ions along the surface normal for the two dominant orientations were calculated. The results are shown in Fig. 7. Here, the orientation angle (θ) is defined as the angle between the surface normal and the direction of electric dipole.^{29, 35, 36, 56} As can be seen, when phosphate ions are added, at least one counterion layer forms near the NH₂-SAM surface. The adsorption starting from orientation O4 has

a relatively narrower distribution and leads to more phosphate ions being adsorbed onto the surface than those for orientation O1. When no protein is added, HPO₄²⁻ is more significantly adsorbed to the positively charged surface than H₂PO₄⁻. For Cyt-c adsorption starting from orientation O4, a similar distribution of the phosphate ions is observed; while for Cyt-c adsorption starting from orientation O1, H₂PO₄⁻ is more significantly adsorbed to the NH₂-SAM surface than HPO₄²⁻ and multiple peaks are observed because the strong phosphate binding sites of Cyt-c are far away from the surface. Therefore, the HPO₄²⁻ counterion layer facilitates the adsorption of Cyt-c with the lysine patch and the heme group being close to the surface, while the H₂PO₄⁻ counterion layer facilitates the adsorption of Cyt-c with the lysine patch and the heme group being far away from the surface. Compared with Fig. 4b, it can be found that Cyt-c adsorbed with orientation O1 weakens the adsorption of phosphate ions onto the NH₂-SAM. This is caused by the competitive binding of the lysine residues of Cyt-c, which mainly locate near the heme crevice, with the phosphate ions.

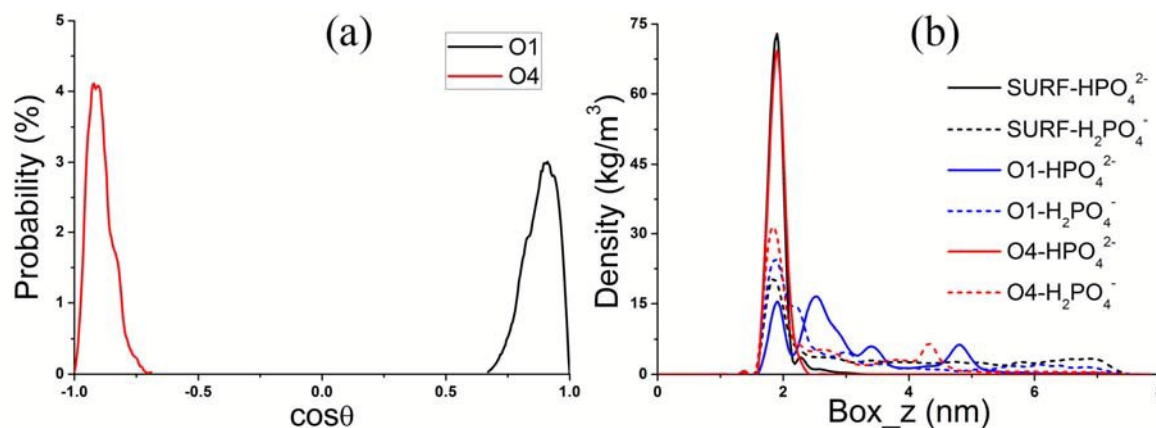


Fig. 7 For the 0.058 M phosphate concentration, (a) orientation distribution of Cyt-c adsorbed on the NH₂-SAM surface, and (b) density profile of phosphate ions along the surface normal of NH₂-SAM for the two dominant orientations.

Binding Sites. To explore the key residues responsible for the adsorptions in the presence of a low phosphate concentration, charged residues containing atoms that are within 0.35 nm of the surface were picked out. The results for the two dominant orientations at the end of the MD simulations are shown in Fig. 8. The adsorption starting from orientation O1 leads to Asp2, Glu4, Lys60, Glu61, Glu62, Glu92, Asp93, Lys99, Lys100, and Glu104 being in contact with the surface. This orientation is similar with that reported for Cyt-c adsorbed on the NH₂-SAM.^{12, 13} It is obvious that most of these residues are negatively charged (Asp and Glu). After a careful look at the adsorption configuration (Fig. 8a), we can find that the adsorption of Lys60 and Lys100 is mediated by the phosphate ions. As has been discussed in Section 3.1, the contact residues Lys60 and Lys100 are among the top ten residues that have strong affinity to the phosphate ions.

On the other hand, the adsorption starting from orientation O4 leads to Lys13, Lys25, Lys27, Lys72, Lys79, Lys86, and Lys87 being in contact with the surface. These

binding sites are similar with those reported for Cyt-c adsorbed on the COOH-SAM.⁹⁻¹¹ After a further observation, we can find that all the residues are positively charged, and the adsorption of these residues is mainly mediated by phosphate ions. This results in the formation of a counterion layer of phosphate ions near the surface (as marked out by the red box in Fig. 8b), which overcompensates the partial positive charges of the surface. Thus, it shows characters of negatively charged surface similar to the COOH-SAM. Furthermore, the contact residues Lys13, Lys25, Lys27, Lys86, and Lys87 are among the top ten residues that have strong affinity to phosphate ions, especially Lys86 and Lys87. This in turn leads to more phosphate ions to be adsorbed onto the surface, as revealed by the higher density of phosphate ions near the NH₂-SAM surface for Cyt-c adsorbed with orientation O4 (Fig. 7b) than that in bulk solution (Fig. 4b).

Interaction Energies. To further investigate the driving forces responsible for adsorption, the interaction energies between some contact residues^{24, 35} of Cyt-c and the NH₂-SAM were calculated, and the results are also depicted in Fig. 8. It is

obvious that the adsorption starting from orientation O1 is mainly attributed to the electrostatic attractions of the negatively charged Asp2 and Glu104 (Fig. 8c), especially the latter, whose net charge is $-2e$ because it locates at the C-terminal. Surprisingly, the positively charged Lys99 also has a strong electrostatic attraction with the surface. With a careful look, we find that this residue is the nearest one to the surface. It inserts into the gap of four nearby neutral amino groups, and the strong electrostatic interaction mainly results from the attractions between the nitrogen atoms and the

hydrogen atoms. However, the electrostatic interaction for the adsorption starting from orientation O4 (-51 kJ/mol) is much weaker than that for orientation O1 (-397 kJ/mol). In contrast, the van der Waals interaction for O4 (-140 kJ/mol) is stronger than that for O1 (-75 kJ/mol). For Lys27, Lys72 and Lys86, it even shows repulsive interactions (Fig. 8d). As HPO_4^{2-} can simultaneously form salt bridges with a lysine residue and a charged amino group of the $\text{NH}_2\text{-SAM}$, it is the phosphate layer that drives these lysine residues to the surface.

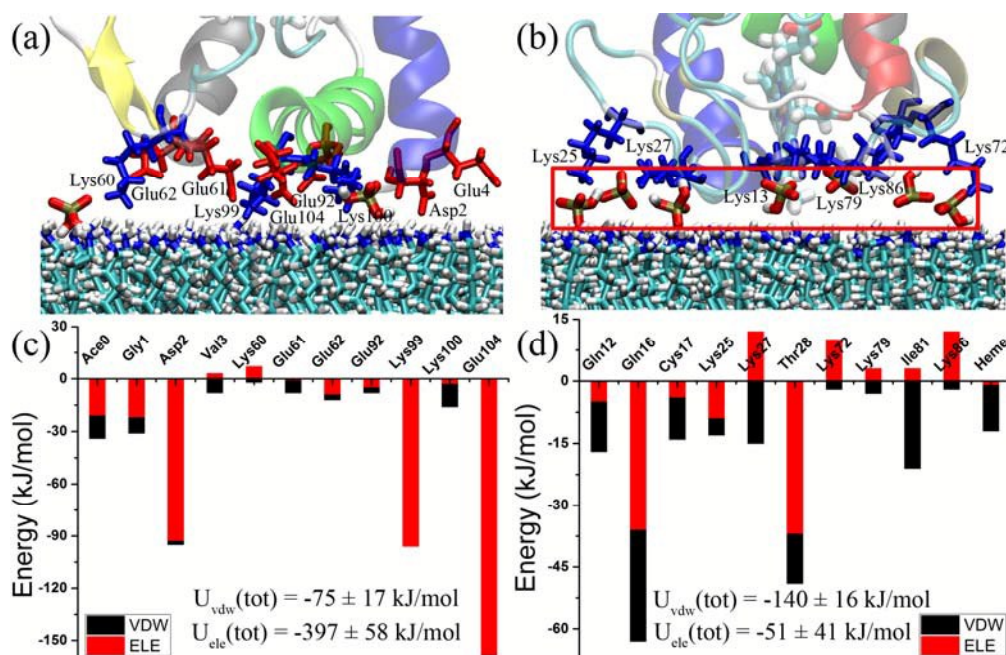


Fig. 8 The two dominant adsorption orientations of Cyt-c on the $\text{NH}_2\text{-SAM}$ surface under the low phosphate concentration (a, b) and the corresponding interaction energies between some contact residues and the surface (c, d). The display modes are the same as that shown in Fig. 5 and the phosphate layer is marked out by a red box.

Protein Conformation. To inspect the structural stability of Cyt-c adsorbed on the $\text{NH}_2\text{-SAM}$, root-mean-square deviation (RMSD) of Cyt-c's backbone atoms were calculated. Furthermore, the simulated structures of Cyt-c on $\text{NH}_2\text{-SAM}$ surface were superimposed on its crystal structure by using VMD.⁵¹ These results are shown in Fig. 9. It is clear that no significant differences are observed between the crystal structure and the simulated structures, which indicate that the crystal structure of Cyt-c is well preserved within the time scale of MD simulations when adsorbed on the $\text{NH}_2\text{-SAM}$ under different phosphate concentrations. This agrees well with those observed in the experiments.⁷ It can be found that the $\Omega 1$ loop (residues 20-30) of Cyt-c has a relatively higher mobility for Cyt-c under the high phosphate concentration. The flexibility of this region has been noticed in some previous studies.^{15, 19, 57} These have been ascribed to the disappearing of the h-bonded turn in this segment, which results in a larger flexibility of these residues.⁵⁸

To quantitatively describe the conformation changes of Cyt-c, the averaged properties such as radius of gyration (R_g), eccentricity, root-mean-square deviation (RMSD) of backbone atoms, and dipole moment of Cyt-c adsorbed on $\text{NH}_2\text{-SAM}$ and in bulk solution were calculated, and the results

were summarized in Table 2. Through a careful comparison, it can be found that the properties of Cyt-c's crystal and solution structure agree well with those calculated by Zhou et al.¹⁸ All the RMSD values are within 1.5 \AA , which indicates that the secondary structure of Cyt-c is well preserved during the adsorptions.¹⁹ The RMSD, R_g , and eccentricity of Cyt-c on the $\text{NH}_2\text{-SAM}$ are comparable with those of crystal structure and in bulk solution. Notably, the RMSD value of Cyt-c on the $\text{NH}_2\text{-SAM}$ for the low phosphate concentration is even lower than that in bulk solution, indicating the adsorption of Cyt-c on this surface helps to preserve its native structure. The same phenomenon can also be found in some previous works,^{59, 60} which may be ascribed to the restriction of the free movement of protein side chain caused by the charged surface. The dipole moment of Cyt-c in bulk solution (251 D) is very close to that of its crystal structure (255 D). However, this value is slightly larger for Cyt-c adsorbed on the positively charged $\text{NH}_2\text{-SAM}$. This is in accordance with the previous simulation results^{14, 18, 19} that the charged surface (such as COOH-SAM) tends to increase the dipole moment of the adsorbed protein. With a careful observation, we can find that the dipole direction and the heme plane of Cyt-c are almost perpendicular to the $\text{NH}_2\text{-SAM}$ surface for all the six

final adsorption configurations under the low phosphate concentration, while they are relatively random for the high

phosphate concentration.

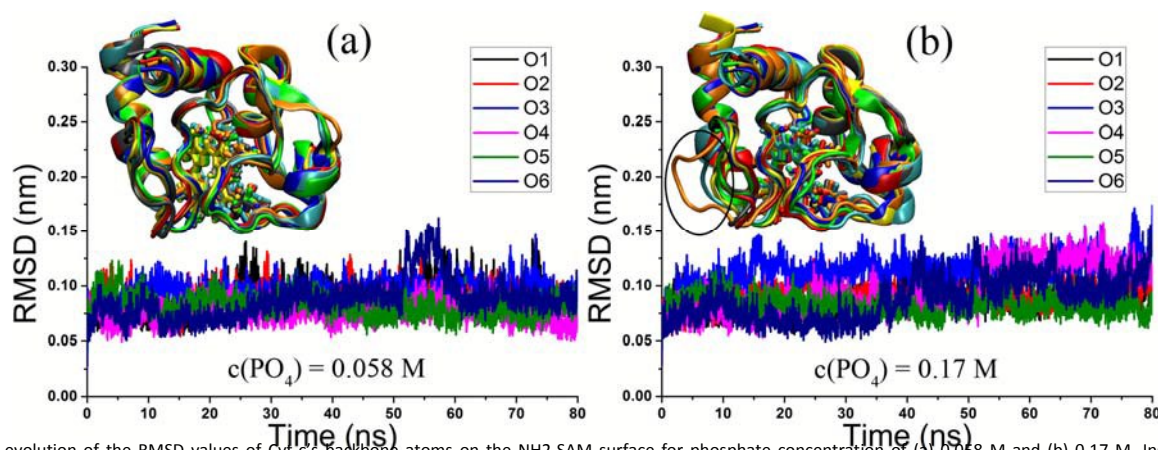


Fig. 9. Time evolution of the RMSD values of Cyt-c's backbone atoms on the NH₂-SAM surface for phosphate concentration of (a) 0.058 M and (b) 0.17 M. Inset: simulated structure of Cyt-c on NH₂-SAM surface superimposed on its crystal structure.

Table 2 Averaged Properties of Cyt-c in Bulk Solution and Adsorbed on the NH₂-SAM Surface

System	Orientation angle	Heme tilt angle (deg)	R_g (Å)	Eccentricity	RMSD (Å)	Dipole moment (D)	
Crystal	-	-	12.64	0.144	-	255	
Bulk	-	-	12.87	0.149	1.13	251 ± 29	
0.058 M	O1	0.88 ± 0.05	88 ± 7	12.89	0.144	1.07	277 ± 41
	O2	0.94 ± 0.05	93 ± 9	12.87	0.149	0.93	295 ± 33
	O3	0.88 ± 0.07	97 ± 10	12.86	0.139	0.98	294 ± 25
	O4	-0.89 ± 0.05	101 ± 4	12.80	0.143	0.73	268 ± 27
	O5	0.91 ± 0.06	87 ± 8	12.83	0.142	0.78	294 ± 26
	O6	0.93 ± 0.04	89 ± 6	12.88	0.144	0.88	295 ± 30
0.17M	O1	0.90 ± 0.07	95 ± 5	12.89	0.140	0.90	297 ± 30
	O2	0.07 ± 0.17	161 ± 8	12.87	0.145	0.96	274 ± 25
	O3	-0.77 ± 0.06	41 ± 5	12.86	0.137	1.22	304 ± 26
	O4	-0.80 ± 0.06	98 ± 4	12.88	0.143	1.24	284 ± 26
	O5	-0.24 ± 0.11	120 ± 3	12.76	0.145	0.81	286 ± 24
	O6	0.02 ± 0.10	33 ± 3	12.85	0.143	1.04	294 ± 31

3.4. Explanations for the contradictory results in experiments

Previous experiments have shown conflicting results regarding to the adsorption and the ET property for Cyt-c on the positively charged surfaces. In this work, we can find that Cyt-c is incapable to bind efficiently to the NH₂-SAM with the addition of chloride, while phosphate can promote its adsorption. Therefore, no stable Cyt-c adsorption should be observed on the positively charged surfaces in pure water or with the addition of chloride^{7, 21}. The detection of Cyt-c adsorption^{7, 12, 13, 20} is due to the addition of the phosphate buffer saline. The experiment results have shown that the amount of adsorbed Cyt-c will decrease with the further increase of phosphate concentration.⁷ As we have shown here, when the phosphate concentration is high, the phosphate and sodium ions will aggregate to form clusters. This may affect the spread of phosphate on the surface, which will result in the decrease of Cyt-c adsorption. It has to be mentioned that, in experiments, the proton is more likely to be shared by multiple NH₂ groups and/or water molecules

and be able to transport. However, in our simulations, the protons are assigned to certain NH₂ groups and cannot transport to other NH₂ groups or water molecules. Therefore, the charge delocalization and transportation may also affect the simulated results.

From our simulations, we can find that under a low phosphate concentration, Cyt-c adsorbs on the NH₂-SAM surface mainly through two opposite orientations. One is similar to that characterized by SERS,¹² or by ToF-SIMS and SFG¹³ for Cyt-c adsorbed on the amino-terminated SAMs. This orientation points the heme group far away from the surface and is not conducive to its ET property. The other orientation is similar to that for Cyt-c on COOH-SAM.⁹⁻¹¹ For this orientation, the distance between the central iron of heme and the surface is about 9.0 Å, which is even smaller than that for the COOH-SAM (about 10.6 Å).^{19, 23} The minimum distance between heme and the surface (about 2.3 Å) is also less than that for the COOH-SAM (about 4.3 Å). Therefore, we can observe direct ET dynamics for Cyt-c adsorbed on the NH₂-SAMs.⁷ For the N⁺(CH₃)₃-SAM, as the surface carries with

strong positive charges, it can attract more chloride³⁰ or phosphate ions and form a stable counterion layer, which results in the positive charges of the surface being overcompensated and produces a negatively charged interface. Thus, similar redox potentials can be observed for Cyt-c adsorbed on N⁺(CH₃)₃-SAMs and on COOH-SAMs.²⁰ While for the NH₂-SAM, as the degree of protonation of the surface under neutral conditions is relatively low, the surface is weakly charged, which cannot form a stable counterion layer³⁰ and results in two opposite adsorption orientations. Therefore, multiple peaks in the electrochemical measurements can be observed for Cyt-c adsorbed on the NH₂-SAMs.²⁰

4. Conclusions

In this work, MD simulations were performed to study the adsorption behavior of Cyt-c on the NH₂-SAM surface. The effects of chloride and phosphate ions and their concentration on the adsorption were also studied. The results reveal that phosphate can bind specifically to certain residues of Cyt-c, especially Lys86 and Lys87. The chloride ions do not significantly adsorb onto the NH₂-SAM surface, and the increase of ion concentration has little impact on the distribution of chloride ions. However, the phosphate ions are more inclined to bind to the NH₂-SAM surface. When the phosphate concentration is low, HPO₄²⁻ has a stronger affinity to the surface than H₂PO₄⁻. At a relatively high concentration, H₂PO₄⁻, HPO₄²⁻, and Na⁺ will aggregate to form a cluster structure with a specific arrangement.

When chloride ions are added, Cyt-c cannot adsorb on the NH₂-SAM surface at the chloride concentration of 0.05 M. When the chloride concentration is increased to 0.15 M, Cyt-c moves close and away from the surface, exhibiting a behavior of reversible adsorption. When phosphate ions are added, Cyt-c can easily adsorb onto the NH₂-SAM surface for both the low and high concentrations. Under a low phosphate concentration, Cyt-c adsorbs on the NH₂-SAM mainly through two opposite orientations. One is similar to that characterized by SERS, or by ToF-SIMS and SFG for Cyt-c adsorbed on the NH₂-SAMs. This orientation points the heme group far away from the surface and is not conducive to its ET property. The other orientation is similar to that for Cyt-c on COOH-SAM; the distance between the central iron of heme and the surface is about 9.0 Å, which is even smaller than that for the COOH-SAM (about 10.6 Å). The adsorption is mainly mediated by phosphate, which leads to more phosphate ions adsorbed onto the surface. At a high phosphate concentration, H₂PO₄⁻, HPO₄²⁻, and Na⁺ will aggregate to form a cluster structure, which leads to the adsorption orientation of Cyt-c being relatively random. For all cases, the crystal structure of Cyt-c is well kept, which agrees well with the experimental results. This work may contribute to the design of Cyt-c-based bioelectronic devices, and provide some guidance for the regulation of ions in enzyme immobilization.

Acknowledgements

This work is funded by the National Key Basic Research Program of China (No. 2013CB733500), National Natural Science Foundation of China (Nos. 21376089 and 91334202), Guangdong Science Foundation (No. 2014A030312007) and the Fundamental Research Funds for the Central Universities (SCUT-2015ZP033). The computational resources for this project are provided by SCUTGrid at South China University of Technology.

Notes and references

- 1 G. Gilardi and A. Fantuzzi, *Trends Biotechnol.*, 2001, **19**, 468-476.
- 2 T. S. Wong and U. Schwaneberg, *Curr. Opin. Biotechnol.*, 2003, **14**, 590-596.
- 3 J. J. Davis, D. A. Morgan, C. L. Wrathmell, D. N. Axford, J. Zhao and N. Wang, *J. Mater. Chem.*, 2005, **15**, 2160-2174.
- 4 Y. H. Wu and S. S. Hu, *Microchim. Acta*, 2007, **159**, 1-17.
- 5 T. Noll and G. Noll, *Chem. Soc. Rev.*, 2011, **40**, 3564-3576.
- 6 S. Prabhulkar, H. Tian, X. Wang, J.-J. Zhu and C.-Z. Li, *Antioxid. Redox Signaling*, 2012, **17**, 1796-1822.
- 7 D. A. Capdevila, W. A. Marmisolle, F. J. Williams and D. H. Murgida, *Phys. Chem. Chem. Phys.*, 2013, **15**, 5386-5394.
- 8 M. Fedurco, *Coord. Chem. Rev.*, 2000, **209**, 263-331.
- 9 S. R. Lin, X. E. Jiang, L. X. Wang, G. H. Li and L. P. Guo, *J. Phys. Chem. C*, 2012, **116**, 637-642.
- 10 K. Ataka and J. Heberle, *J. Am. Chem. Soc.*, 2004, **126**, 9445-9457.
- 11 J. Xu and E. F. Bowden, *J. Am. Chem. Soc.*, 2006, **128**, 6813-6822.
- 12 Q. Yu and G. Golden, *Langmuir*, 2007, **23**, 8659-8662.
- 13 J. Baio, T. Weidner, D. Ramey, L. Pruzinsky and D. Castner, *Biointerphases*, 2013, **8**, 1-8.
- 14 D. A. Paggi, D. F. Martín, A. Kranich, P. Hildebrandt, M. A. Martí and D. H. Murgida, *Electrochim. Acta*, 2009, **54**, 4963-4970.
- 15 D. Alvarez-Paggi, M. A. Castro, V. Tórtora, L. Castro, R. Radi and D. H. Murgida, *J. Am. Chem. Soc.*, 2013, **135**, 4389-4397.
- 16 D. Alvarez-Paggi, W. Meister, U. Kuhlmann, I. Weidinger, K. Tenger, L. Zimányi, G. Rákhely, P. Hildebrandt and D. H. Murgida, *J. Phys. Chem. B*, 2013, **117**, 6061-6068.
- 17 B. Trzaskowski, F. Leonarski, A. Les and L. Adamowicz, *Biomacromolecules*, 2008, **9**, 3239-3245.
- 18 J. Zhou, J. Zheng and S. Y. Jiang, *J. Phys. Chem. B*, 2004, **108**, 17418-17424.
- 19 D. Alvarez-Paggi, D. F. Martín, P. M. DeBiase, P. Hildebrandt, M. A. Martí and D. H. Murgida, *J. Am. Chem. Soc.*, 2010, **132**, 5769-5778.
- 20 X. X. Chen, R. Ferrigno, J. Yang and G. A. Whitesides, *Langmuir*, 2002, **18**, 7009-7015.
- 21 P. S. Jensen, Q. Chi, F. B. Grummen, J. M. Abad, A. Horsewell, D. J. Schiffrin and J. Ulstrup, *J. Phys. Chem. C*, 2007, **111**, 6124-6132.
- 22 A. Hung, S. Mwenifumbo, M. Mager, J. J. Kuna, F. Stellacci, I. Yarovsky and M. M. Stevens, *J. Am. Chem. Soc.*, 2011, **133**, 1438-1450.
- 23 Y. Xie, Y. Pan, R. Zhang, Y. Liang and Z. Li, *Appl. Surf. Sci.*, 2015, **326**, 55-65.
- 24 C. Peng, J. Liu and J. Zhou, *J. Phys. Chem. C*, 2015, **119**, 20773-20781.
- 25 J. Petrović, R. A. Clark, H. Yue, D. H. Waldeck and E. F. Bowden, *Langmuir*, 2005, **21**, 6308-6316.
- 26 S. Pasche, J. Vörös, H. J. Griesser, N. D. Spencer and M. Textor, *J. Phys. Chem. B*, 2005, **109**, 17545-17552.

- 27 E. Palecek and V. Ostatna, *Chem. Commun.*, 2009, DOI: 10.1039/B822274F, 1685-1687.
- 28 R. Schlapak, D. Armitage, N. Saucedo-Zeni, W. Chrzanowski, M. Hohage, D. Caruana and S. Howorka, *Soft Matter*, 2009, **5**, 613-621.
- 29 Y. Xie, J. Zhou and S. Y. Jiang, *J. Chem. Phys.*, 2010, **132**, 065101.
- 30 J. Liu, C. Peng, G. Yu and J. Zhou, *Langmuir*, 2015, **31**, 10751-10763.
- 31 G. W. Bushnell, G. V. Louie and G. D. Brayer, *J. Mol. Biol.*, 1990, **214**, 585-595.
- 32 F. Autenrieth, E. Tajkhorshid, J. Baudry and Z. Luthey-Schulten, *J. Comput. Chem.*, 2004, **25**, 1613-1622.
- 33 B. Hess, C. Kutzner, D. van der Spoel and E. Lindahl, *J. Chem. Theory Comput.*, 2008, **4**, 435-447.
- 34 A. D. MacKerell, D. Bashford, Bellott, R. L. Dunbrack, J. D. Evanseck, M. J. Field, S. Fischer, J. Gao, H. Guo, S. Ha, D. Joseph-McCarthy, L. Kuchnir, K. Kuczera, F. T. K. Lau, C. Mattos, S. Michnick, T. Ngo, D. T. Nguyen, B. Prodhom, W. E. Reiher, B. Roux, M. Schlenkrich, J. C. Smith, R. Stote, J. Straub, M. Watanabe, J. Wiórkiewicz-Kuczera, D. Yin and M. Karplus, *J. Phys. Chem. B*, 1998, **102**, 3586-3616.
- 35 C. Peng, J. Liu, D. Zhao and J. Zhou, *Langmuir*, 2014, **30**, 11401-11411.
- 36 J. Liu, C. Y. Liao and J. Zhou, *Langmuir*, 2013, **29**, 11366-11374.
- 37 S. E. Feller and A. D. MacKerell, *J. Phys. Chem. B*, 2000, **104**, 7510-7515.
- 38 B. A. Averill and P. Eldredge, in *Principles of General Chemistry (v. 1.0)*, Creative Commons licensed, 2012, ch. 27, p. 2991.
- 39 R. L. Jungas, *Anal. Biochem.*, 2006, **349**, 1-15.
- 40 W. Yang, Y. Q. Gao, Q. Cui, J. Ma and M. Karplus, *Proc. Natl. Acad. Sci. U. S. A.*, 2003, **100**, 874-879.
- 41 K. Vanommeslaeghe, E. Hatcher, C. Acharya, S. Kundu, S. Zhong, J. Shim, E. Darian, O. Guvench, P. Lopes, I. Vorobyov and A. D. Mackerell, *J. Comput. Chem.*, 2010, **31**, 671-690.
- 42 S. S. Mallajosyula, O. Guvench, E. Hatcher and A. D. MacKerell, *J. Chem. Theory Comput.*, 2011, **8**, 759-776.
- 43 W. L. Jorgensen, J. Chandrasekhar, J. D. Madura, R. W. Impey and M. L. Klein, *J. Chem. Phys.*, 1983, **79**, 926.
- 44 T. J. Piggot, Á. Piñeiro and S. Khalid, *J. Chem. Theory Comput.*, 2012, **8**, 4593-4609.
- 45 P. Bjelkmar, P. Larsson, M. A. Cuendet, B. Hess and E. Lindahl, *J. Chem. Theory Comput.*, 2010, **6**, 459-466.
- 46 W. G. Hoover, *Phys. Rev. A: At. Mol. Opt. Phys.*, 1985, **31**, 1695.
- 47 M. Parrinello and A. Rahman, *J. Appl. Phys.*, 1981, **52**, 7182-7190.
- 48 B. Hess, H. Bekker, H. J. C. Berendsen and J. G. E. M. Fraaije, *J. Comput. Chem.*, 1997, **18**, 1463-1472.
- 49 T. Darden, D. York and L. Pedersen, *J. Chem. Phys.*, 1993, **98**, 10089.
- 50 I. C. Yeh and M. L. Berkowitz, *J. Chem. Phys.*, 1999, **111**, 3155-3162.
- 51 W. Humphrey, A. Dalke and K. Schulten, *J. Mol. Graphics*, 1996, **14**, 33-38.
- 52 N. Osheroff, D. L. Brautigan and E. Margoliash, *Proc. Natl. Acad. Sci. U. S. A.*, 1980, **77**, 4439-4443.
- 53 K. Onuma and A. Ito, *Chem. Mater.*, 1998, **10**, 3346-3351.
- 54 A. Oyane, K. Onuma, T. Kokubo and A. Ito, *J. Phys. Chem. B*, 1999, **103**, 8230-8235.
- 55 G. B. Yu, J. Liu and J. Zhou, *J. Phys. Chem. B*, 2014, **118**, 4451-4460.
- 56 J. Zhou, S. F. Chen and S. Y. Jiang, *Langmuir*, 2003, **19**, 3472-3478.
- 57 W. Pulawski, S. Filipek, A. Zwolinska, A. Debinski, K. Krzysko, R. Garduño-Juárez, S. Viswanathan and V. Renugopalakrishnan, *Eur. Biophys. J.*, 2013, **42**, 291-300.
- 58 M. E. Siwko and S. Corni, *Phys. Chem. Chem. Phys.*, 2013, **15**, 5945-5956.
- 59 J. Zhao, Q. Wang, G. Liang and J. Zheng, *Langmuir*, 2011, **27**, 14876-14887.
- 60 J. Liu, G. Yu and J. Zhou, *Chem. Eng. Sci.*, 2015, **121**, 331-339.

75